

P–T–t evolution of an Early Silurian medium-grade shear zone on the west side of the Famatinian magmatic arc, Argentina: Implications for the assembly of the Western Gondwana margin

B. Castro de Machuca^{a,b,*}, G. Arancibia^c, D. Morata^d, M. Belmar^d, L. Previley^{a,b}, S. Pontoriero^b

^a CONICET, Argentina

^b Instituto de Geología, FCEFN, Universidad Nacional de San Juan. Av. Ignacio de la Roza y Meglioli, C.P. 5407 Rivadavia, San Juan, Argentina

^c Laboratorio Servicio Nacional de Geología y Minería, Avenida Til-Til 1993-Ñuñoa, Santiago, Chile

^d Departamento de Geología, Universidad de Chile, Plaza Ercilla 803, Santiago, Chile

Abstract

The geodynamic evolution of the proto-Andean margin of Gondwana during the Paleozoic was characterized by repeated subduction processes associated with the docking of several terranes, including the Cuyania–Precordillera terrane and the Chilenia terrane, and the development of the calc–alkaline Famatinian continental magmatic arc. In the Sierra de La Huerta (30°56′–31°29′ S and 67°17′–67°32′ W), at the southwestern end of the Western Sierras Pampeanas, some mafic to ultramafic igneous bodies belonging to the Famatinian arc were affected by regional metamorphism of the medium-pressure granulite facies (7–7.5 kbar, ≈850 °C). After this regional metamorphism, local mylonitization under amphibolite facies along discrete NW–SE to NNW–SSE striking ductile shear zones occurred. A ⁴⁰Ar/³⁹Ar plateau age of 432±4 Ma was obtained on rather homogeneous hornblende porphyroclasts from a metagabbro mylonite. The textures and mineral chemistry of the mylonitized metagabbro allow its *P–T–t* evolution from magmatic crystallization to mylonitization to be constrained. Geochronological data obtained from mylonite provide evidence that orogenesis was active at least until the Early Silurian. This deformational event would have been related to uplift and decompression during the later stages of the orogenesis, probably associated with the accretion of the Precordillera terrane to the southwestern Gondwana margin.

Keywords: Metagabbroic mylonites; *P–T* path; ⁴⁰Ar/³⁹Ar dating; Sierra de La Huerta; Famatinian Orogeny; Argentina

1. Introduction

The geodynamic evolution of the proto-Andean margin of Gondwana in Paleozoic times was characterized by repeated subduction processes associated with the docking of several terranes (Ramos et al., 1998; Pankhurst and Rapela, 1998; Rapela et al., 1998; Kleine et al., 2004; Ramos, 2004). In the area of present-day central Chile and central Argentina, the Cuyania (Precordillera) and the Chilenia terranes are considered to have been amalgamated to Gondwana during the Paleozoic (Ramos

* Corresponding author. Instituto de Geología, FCEFN, Universidad Nacional de San Juan. Av. Ignacio de la Roza y Meglioli, C.P. 5407 Rivadavia, San Juan, Argentina. Tel./fax: +54 264 4265103.

E-mail address: bcastro@unsj-cuim.edu.ar (B. Castro de Machuca).

et al., 1986; Ramos, 1988; Astini et al., 1995; Thomas and Astini, 1996). The Valle Fértil lineament along the western foothills of the Sierras de Valle Fértil–La Huerta is considered the present eastern boundary of the Cuyania terrane (Introcaso et al., 2004).

Rocks associated with Early Paleozoic subduction activity along the western margin of Gondwana are widely distributed in the west part of the Sierras Pampeanas of central Argentina and are generally referred to as the Famatinian magmatic arc (e.g. Pankhurst and Rapela, 1998; Rapela et al., 1998). The latter lies between the autochthonous Pampean orogen (Mid- to Late Proterozoic–Mid-Cambrian) which constitutes the foreland, on the east, and the allochthonous Precordillera terrane (a “Grenvillian” basement covered by non-metamorphosed to weakly metamorphosed Cambrian–Devonian deposits, Keller et al., 1998) to the west. The arc was developed along the

Gondwana margin during the Early Ordovician and represents the subduction stage that preceded the collision of the Precordillera terrane with the proto-Pacific margin of South America during the Middle Ordovician (Pankhurst et al., 1998).

Previous studies show that the Famatinian arc is a calc-alkaline subduction-related continental magmatic arc that was active between 470 and 490 Ma (e.g. Pankhurst et al., 1998, 2000, and references therein). Regional metamorphism at ca. 460 Ma (Casquet et al., 2001a; Baldo et al., 2001; Rapela et al., 2001; Vujovich et al., 2004) was associated with the collision of the Cuyania terrane. Peak metamorphic conditions reaching the granulite facies were attained (e.g. Baldo et al., 2001) and associated deformation was responsible for the NNW–SSE foliation in the crystalline basement of the Sierras de Valle Fértil–La Huerta and Las Imanas.

After regional metamorphism, local mylonitization along discrete NW–SE to NNW–SSE ductile shear zones occurred in this area (Murra and Baldo, 2001; Castro de Machuca et al., 2004, 2005). According to Murra (2004) this event resulted from uplift and decompression during the later stages of the orogenesis (452–459 Ma), probably associated with the accretion of the Precordillera terrane and representing the last metamorphic event during the construction of the Famatinian arc. The final stage in the evolution of the proto-Andean Gondwana margin consisted of intra-plate magmatism to the east of the arc that took place in Devonian–Carboniferous times (e.g. Dahlquist et al., 2006, and references therein). At this point, the Paleozoic geological development of the Sierras Pampeanas ceased, indicating the stability of the new continental margin, until the start of the Andean cycle in Cretaceous times (Pankhurst and Rapela, 1998).

In this study we focus on mylonites that developed from mafic–ultramafic protoliths cropping out in the Sierra de La Huerta (30°56′–31°29′ S and 67°17′–67°32′ W), at the southwestern end of the Western Sierras Pampeanas (Fig. 1). P – T estimations and the $^{40}\text{Ar}/^{39}\text{Ar}$ geochronology of this ductile deformation event were determined with the aim of constraining the end of the Famatinian arc-building and, consequently, to improve the geological models proposed for the evolution of the western Gondwana margin.

2. Geological setting

The Sierras de Valle Fértil–La Huerta and Las Imanas, the westernmost parts of the Famatinian belt, constitute a morphostructural lineament of pre-Andean high-grade crystalline basement. The latter consists of Upper Proterozoic–Lower Paleozoic metamorphic rocks (metapelitic gneisses, migmatites, marbles and amphibolites), intruded by calc-alkaline metaluminous granodiorites, tonalites, diorites, gabbros, ultramafic rocks and younger granites and pegmatites (Castro de Machuca et al., 1996, and references therein) in Early Ordovician times (468–499 Ma, Pankhurst et al., 2000). Both igneous and metamorphic units were later deformed and transformed into mylonites and ultramylonites along ductile shear zones resulting from a non-coaxial deformation event, showing a retrograde high-grade metamorphic paragenesis of medium-grade minerals

(e.g. Murra and Baldo, 2001; Murra, 2004; Castro de Machuca et al., 2005).

Granodiorites and tonalites are dominant along the eastern flank of the Sierra de Valle Fértil, but lesser amounts of mafic and ultramafic rocks are also found. Tonalites and diorites constitute the more abundant rocks at the eastern side of the Sierra de La Huerta, although gabbroic and ultramafic rocks are locally important. The abundance of intermediate and mafic–ultramafic rocks at the southernmost outcrop could suggest a deeper level (“root”) of exposure of the Famatinian magmatic arc (Castro de Machuca et al., 2002).

Within the Famatinian arc, the different igneous lithologies, including septa of paragneisses, marbles and amphibolites, underwent lower granulite (hornblende–granulite) facies metamorphism. The association of coronitic metagabbros–metagabbrobrorites and ultramafic rocks (peridotites, pyroxenites, hornblendites and lherzolites) with quartz metadiorites, metatonalites and metagranodiorites is common (see also Murra and Baldo, 2006, and references therein). Regional metamorphism, with peak T at 863–930 °C and P between 7–8 kbar (Castro de Machuca et al., 2004), resulted from collision of the Pampia and Cuyania terranes (Chernicoff and Ramos, 2003) and was accompanied by the development of a NNW–SSE penetrative foliation. U–Pb SHRIMP ages on zircon overgrowths indicate a ca. 465 Ma age for the peak of the medium to high-grade regional metamorphism in the area (e.g. Rapela et al., 2001; Baldo et al., 2001; Casquet et al., 2001a; Vujovich et al., 2004). South of the Sierra de La Huerta, a Sm–Nd (Grt+Pl+whole-rock) age of 464.6 ± 4.5 Ma from a migmatitic gneiss ($T=720$ – 790 °C, $P=6.5$ – 7 kbar) in the Sierra de Las Imanas, was also interpreted as the age of metamorphism (Galindo et al., 2004). Lower P – T values obtained by these authors suggest that the migmatitic gneiss belongs to higher crustal levels than metagabbrobrorites and metagabbros from elsewhere in the Sierra de La Huerta.

Post-regional metamorphism ductile shear zones developed after regional high-grade (granulite facies) protoliths. In the study area, centimetre to meter wide, penetrative NW–SE to NNW–SSE striking mylonite zones (Fig. 1) dip steeply to the NE with a down-dip stretching and mineral lineation (average pitch 85° NW). Displacement in mylonite zones is predominantly reverse but a minor dextral strike–slip component of displacement is also found. Kinematic analysis yields consistent picture of tectonic displacement toward the W–SW. Mylonites are well developed in metagabbroic rocks but also occur in other lithologies. Mylonitic foliation is characteristically defined by the development of mafic and felsic layers (striped texture, Passchier and Trouw, 1996) in spatial transition between coarse-grained undeformed metagabbros and fine-grained mylonitic bands. Layering, foliation and lineation are strongly developed (Fig. 2).

3. Sampling and analytical methods

3.1. Mineral chemistry

From a total of ninety-six collected samples of undeformed and deformed metagabbros, optical microscope and back-

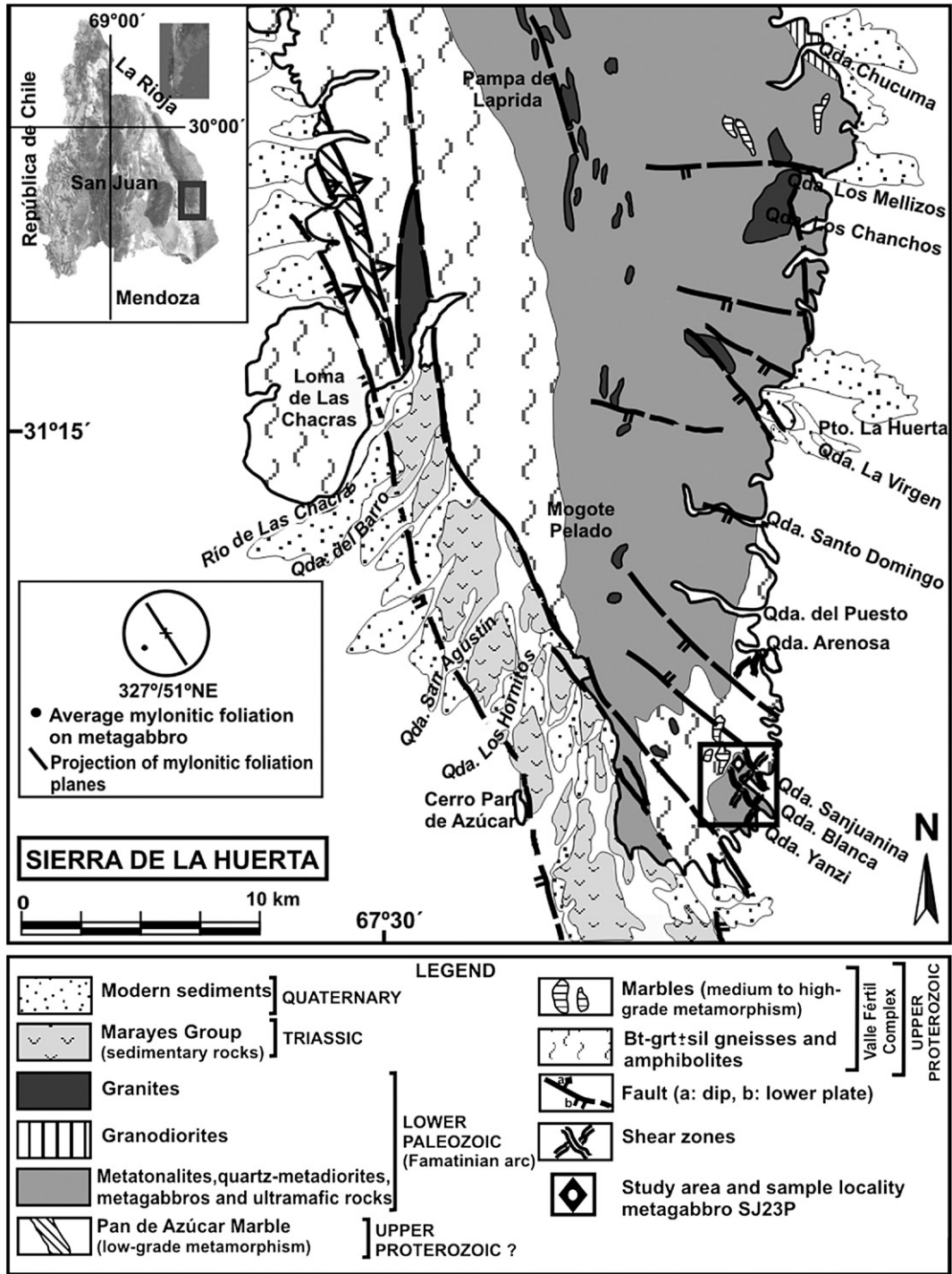


Fig. 1. Simplified geological map of the Sierra de la Huerta showing the location of the study area and dated sample (modified from Vujovich et al., 1996).

scattered scanning electron microscope images were obtained from seven representative oriented sections parallel to the lineation and perpendicular to the foliation (samples BLM9, BLM9b, BM8b, BM7, ARM22, BLM10 and SJ23P). These selected samples were used for microstructural and microprobe studies. Mineral chemistry was determined by electron microprobe analyses (EMPA) on polished and carbon-coated (≈ 10 nm) thin sections. Spot chemical analyses were carried

out in a CAMECA SU-30 SEM-probe (Departamento de Geología, Universidad de Chile, 10 nA, 15 kV, 2 μ m beam size and 10 s acquisition time). Natural minerals were used as standards and ZAF correction program applied. Previous EMPA data from eight undeformed olivine-bearing metagabbros and ultramafic rocks (samples S1, S2, R6, RSJ14, J14, AR2, R2 and R4, Castro de Machuca et al., 2002) were also used. Representative microprobe analyses are given in Table 1.

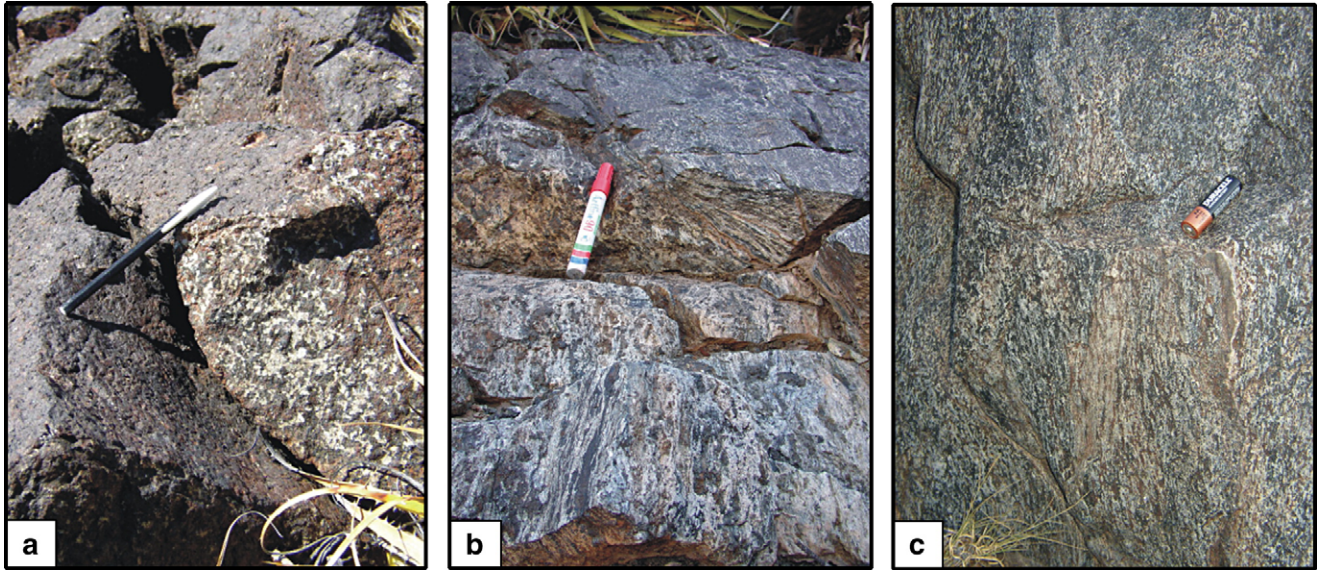


Fig. 2. Sequence of metagabbro outcrops showing a gradation from undeformed coarse-grained metagabbro (a) with increasing deformation to tectonically layered striped metagabbro (b) and intensely deformed fine-grained metagabbro mylonite (c). All photographs are from a NNW–SSE trending ductile shear zone in Quebrada Sanjuanina, southeastern Sierra de La Huerta.

3.2. $^{40}\text{Ar}/^{39}\text{Ar}$ procedures

One sample of mylonitized metagabbro (SJ23P) was chosen for $^{40}\text{Ar}/^{39}\text{Ar}$ dating. Sample preparation and $^{40}\text{Ar}/^{39}\text{Ar}$ amphibole analysis were carried out in the Laboratorio de Geocronología of the Servicio Nacional de Geología y Minería (Chile). Amphibole was separated by hand picking under a binocular microscope from a 250–180 μm fraction. Separated minerals were cleaned in distilled water for 15 min and dried. Details of analytical procedures and irradiation are given in Arancibia et al. (2006). After irradiation the sample was cooled for three months and the J -factor value was 0.001154 ± 0.0000054 (Table 2). Blanks obtained during the analysis were as follows: $^{40}\text{Ar} = 7.42 \times 10^{-17}$, $^{39}\text{Ar} = 4.51 \times 10^{-19}$, $^{38}\text{Ar} = 7.63 \times 10^{-20}$, $^{37}\text{Ar} = 8.13 \times 10^{-19}$, and $^{36}\text{Ar} = 2.44 \times 10^{-19}$ mol.

4. Petrography and mineral chemistry

4.1. Undeformed metagabbros

The mafic–ultramafic bodies associated with the more felsic metaigneous rocks range in size from tens to a few hundred meters, and they are mainly massive, dark-coloured, coarse-grained metagabbros (Fig. 2a). According to modal analyses, these rocks classify as gabbros, gabbronorites and olivine-bearing gabbronorites. In the central parts of these bodies, the rocks display well preserved igneous textures and mineralogy and, in some cases, a rhythmic layering is observed. In contrast, marginal parts of the mafic bodies are strongly recrystallized and primary pyroxenes are almost completely replaced by metamorphic amphibole.

The relic igneous mineralogy is formed mainly by subhedral to anhedral rounded grains, up to 4 mm in size, of almost unzoned Mg-rich olivine (Fo_{81} to Fo_{74} , Table 1), Mg-rich orthopyroxene

($\approx \text{En}_{77}\text{Fs}_{23}$), clinopyroxene ($\text{En}_{44-47}\text{Fs}_{6-8}\text{Wo}_{50-46}$) and subhedral to anhedral anorthite (An_{100-99} , Table 1). Pyroxenes are usually clouded with ilmenite–magnetite schiller inclusions. Petrographic relationships indicate a crystallization order of olivine, plagioclase, orthopyroxene and finally clinopyroxene (frequent inclusions of olivine in orthopyroxene and plagioclase in clinopyroxene), consistent with relatively low-pressure crystallization conditions as previously proposed by Rabbia (1996).

As a consequence of metamorphism, abundant coronas of orthopyroxene ($\text{En}_{82-75}\text{Fs}_{18-24}\text{Wo}_{0-1}$) \pm clinopyroxene ($\text{En}_{47-43}\text{Fs}_{6-8}\text{Wo}_{50-49}$) + Al-rich spinel ($\text{Sp}_{66-43}\text{Hc}_{34-56}$) are present at the olivine–plagioclase contacts (Fig. 3a). Spinel is intergrown with clinopyroxene but is also present as single grains. A granoblastic polygonal texture is often found in relic pyroxenes and plagioclase. All these textures are typical of the granulite facies of metamorphism.

Pleochroic pale green tschermakite and tschermakitic hornblende appear at the outermost rim of these coronas in vermicular symplectitic intergrowths with green spinel (Fig. 3a, b), rimming and replacing pyroxenes, as large oikocrysts enclosing previous minerals and as a medium-grained polygonal mosaic in the matrix. Chemically, these amphiboles are characterized by Al_2O_3 contents ranging from 13.05–15.88 wt.%, Na_2O from 1.14–2.85 wt.%, and relatively low TiO_2 (<0.95 wt.%) contents (Table 1). Chemical variations in the amphiboles are dominated by a tschermakitic-type substitution ($\text{Al}^{\text{IV}} + \text{Al}^{\text{VI}} \leftrightarrow \text{Mg} + \text{Si}$).

4.2. Mylonites

The transition from undeformed metagabbro to highly deformed mylonite occurs over a distance of only a few centimetres (Fig. 2b and c). The most significant changes resulting from mylonitization are decreasing grain-size and

Table 1
Representative composition of mineral phases in undeformed metagabbros (Mgb) and mylonites (Myl) from the Sierra de la Huerta

Sample	R6	J14	S2	BLM9	SJ23P	SJ23P	R2	J14	R2	BLM9	BLM9	SJ23P	R2	SJ23P	R2		
Analysis	3–20	1	2–33	117	3–59	1–82	2–7	7	2–9	114	127	1–63	2–11	3–42	2–1		
Mineral	Ol	Ol	Pl	Pl	Pl	Pl	Cpx	Opx	Opx	Cpx	Opx	Opx	Amp	Amp	Spl		
Rock	Mgb	Mgb	Mgb	Myl	Myl	Myl	Mgb	Mgb	Mgb	Myl	Myl	Myl	Mgb	Myl	Mgb		
SiO ₂	39.28	37.78	41.84	41.68	43.79	52.40	50.53	53.86	53.39	51.26	50.30	50.47	42.41	43.55	FeO	27.61	
TiO ₂	0.01	0.04	0.00	0.03	0.11	0.00	0.19	0.08	0.02	0.16	0.03	0.05	0.53	0.72	V ₂ O ₃		
Al ₂ O ₃	0.00	0.00	37.16	36.17	36.09	29.43	2.99	1.70	3.06	3.17	4.32	2.00	14.30	11.67	TiO ₂	0.04	
Cr ₂ O ₃	0.00	0.00					0.22	0.14	0.01				0.07	0.00	Al ₂ O ₃	52.18	
FeO	18.66	23.66	0.08	0.02	0.14	0.24	4.08	14.52	13.27	4.39	17.31	23.86	7.84	12.62	MnO	0.08	
MnO	0.26	0.29	0.00	0.00	0.00	0.18	0.03	0.31	0.23	0.38	0.36	0.69	0.09	0.14	Cr ₂ O ₃	7.23	
MgO	43.62	38.32	0.11	0.02	0.02	0.00	15.89	28.49	29.45	16.40	28.36	21.37	16.10	13.53	MgO	12.30	
CaO	0.06	0.09	20.49	20.97	19.20	11.72	24.59	0.37	0.48	24.88	0.31	0.32	12.49	11.98	SiO ₂	0.35	
Na ₂ O	0.40	0.00	0.11	0.07	1.28	4.95	0.00	0.00	0.00	0.06	0.02	0.13	1.73	1.27	CaO	0.24	
K ₂ O	0.00	0.00	0.00	0.02	0.05	0.07	0.00	0.00	0.00	0.00	0.00	0.01	0.52	1.23			
SUM	102.29	100.18	99.79	98.97	100.68	98.98	98.52	99.47	99.91	100.71	101.01	98.90	96.08	96.71	SUM	100.03	
N. Ox	4	4	8	8	8	8	6	6	6	6	6	6	23	23		32	
Si	0.983	0.989	1.950	1.962	2.019	2.401	Si	1.874	1.936	1.894	1.858	1.783	1.907	6.102	6.384	Fe ²⁺	4.038
Ti	0.000	0.001	0.000	0.001	0.004	0.000	Al ^{IV}	0.126	0.064	0.106	0.135	0.181	0.089	1.898	1.616	V ³⁺	0.000
Al	0.000	0.000	2.041	2.007	1.961	1.589	Ti	0.005	0.002	0.001	0.004	0.001	0.001	0.057	0.079	Ti	0.007
Cr ³⁺	0.000	0.000	0.000	0.000	0.000	0.000	Al ^{VI}	0.005	0.008	0.022	0.000	0.000	0.000	0.528	0.402	Al	13.573
Fe ²⁺	0.390	0.518	0.003	0.001	0.005	0.009	Fe ³⁺	0.104	0.049	0.082	0.143	0.253	0.103	0.819	0.699	Mn	0.015
Mn ²⁺	0.006	0.006	0.000	0.000	0.000	0.007	Cr	0.006	0.004	0.000	0.000	0.000	0.000	0.008	0.000	Cr	1.262
Mg	1.627	1.495	0.008	0.001	0.001	0.000	Fe ²⁺	0.024	0.389	0.315	0.000	0.271	0.657	0.125	0.848	Mg	4.047
Ca	0.002	0.003	1.023	1.058	0.948	0.575	Mn ²⁺	0.001	0.009	0.007	0.012	0.011	0.022	0.011	0.017	Fe ³⁺	1.152
Na	0.019	0.000	0.010	0.007	0.115	0.440	Mg	0.879	1.526	1.558	0.886	1.499	1.204	3.452	2.955		
K	0.000	0.000	0.000	0.001	0.003	0.004	Ca	0.977	0.014	0.018	0.967	0.012	0.013	1.925	1.882		
							Na	0.000	0.000	0.000	0.004	0.001	0.009	0.483	0.361		
							K	0.000	0.000	0.000	0.000	0.000	0.000	0.095	0.231		
Σcat	3.027	3.011	5.035	5.037	5.056	5.026	Σcat.	4.001	4.002	4.003	4.002	4.011	4.007	15.504	15.474	Σcat.	24.093
Fo	0.81	0.74	99.06	99.29	88.96	56.43	En	44.276	76.771	78.699	44.329	73.267	60.202			Spl	49.96%
Fa	0.19	0.26	0.94	0.62	10.76	43.18	Fs	6.481	22.513	20.379	7.330	26.159	39.144			Hc	49.85%
			0	0.09	0.28	0.39	Wo	49.244	0.717	0.922	48.341	0.574	0.654			Galax	0.18%

Ol: olivine; Pl: plagioclase; Cpx: clinopyroxene; Opx: orthopyroxene; Amp: amphibole; Spl: spinel.

development of foliation. The latter is defined by alternating mafic and felsic mineral-rich bands that result in a striped structure at mesoscopic and microscopic scales (Figs. 2b and 3b). This compositional layering consists of polygonal pyroxene+amphibole-rich and plagioclase-rich bands 1 cm to 0.5 mm wide (Fig. 3b). According to EMPA data, no major differences are found in pyroxenes and amphiboles from undeformed and deformed metagabbros. Porphyroclasts with

a relic coronitic texture are also found, as evidenced by pyroxene cores rimmed by amphibole±spinel coronas (Fig. 3c). Symplectitic intergrowths of clinopyroxene–spinel, characteristic of undeformed metagabbros, are however very scarce.

Where grain-size reduction is more important, the dominant texture is mylonitic, with a few large elongated porphyroclasts (up to 4 mm Ø) immersed in a very fine-grained matrix (Fig. 3c, d, e, f and g). Clino- and orthopyroxene porphyroclasts mainly

Table 2
⁴⁰Ar/³⁹Ar data obtained from amphiboles in metagabbro mylonite (S 31° 23' 43"–W 67° 19' 33") from the Sierra de La Huerta

SJ23P (Amphibole porphyroclasts from mylonitized metagabbro, Quebrada Sanjuanina, Sierra de La Huerta)

Step	Laser power	³⁶ Ar/ ³⁹ Ar	³⁷ Ar/ ³⁹ Ar	³⁸ Ar/ ³⁹ Ar	⁴⁰ Ar*/ ³⁹ Ar	Mol ³⁹ Ar	% ⁴⁰ Ar*	Age (Ma)	(±2σ)
A	5	0.900	10.626	0.066	84.399	0.001	24.10	168.07	4.89
B	10	0.181	8.466	0.050	224.778	0.006	80.90	417.07	1.79
C	12	0.016	7.537	0.085	234.818	0.013	98.10	433.63	1.32
D	14	0.013	8.257	0.074	233.308	0.014	98.50	431.15	1.83
E	16	0.007	7.961	0.078	233.396	0.014	99.30	431.29	0.97
F	18	0.005	8.320	0.091	234.323	0.009	99.50	432.82	1.47
G	20	0.005	8.422	0.081	233.697	0.009	99.60	431.79	1.52
H	25	0.004	8.172	0.077	234.500	0.009	99.70	433.11	1.52
I	30	0.022	8.664	0.072	234.000	0.008	97.40	432.29	1.50

Integrated age=428±4 Ma; J=0.001154±0.0000054.

Plateau age=432±4 Ma (91.1% released gas).

Inverse isochron age=432±2 Ma, n=7.

Data in italics were excluded in isochron analysis. Laser power in watts. ⁴⁰Ar*=radiogenic ⁴⁰Ar.

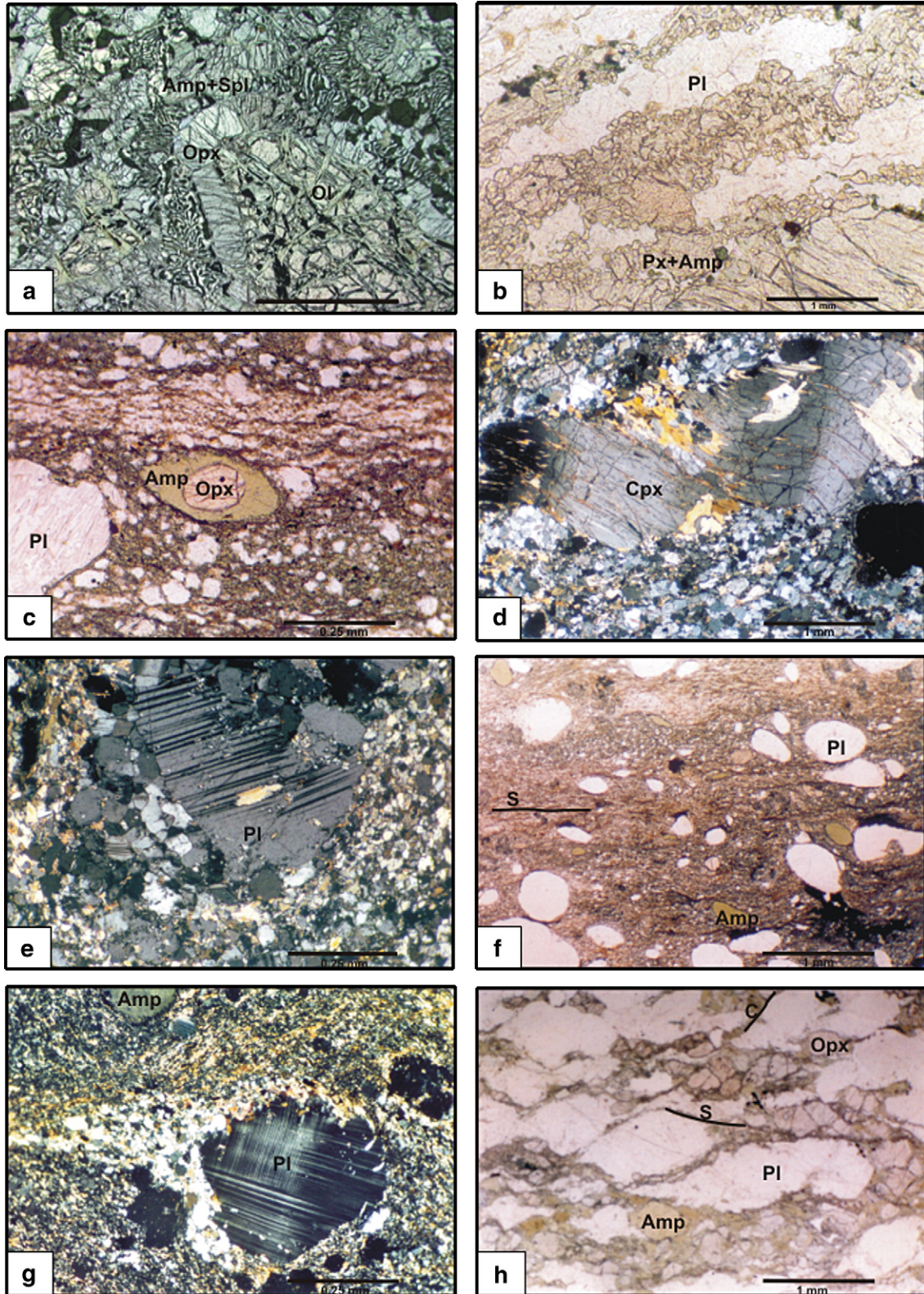


Fig. 3. Microstructures of metagabbros from the Sierra de La Huerta. a) Opx+Cpx+Amp+Al-Spl symplectitic coronas developed at the olivine-plagioclase boundary in undeformed metagabbro (PPL). b) Striped texture composed of millimetric mafic (Cpx±Opx+Amp) and felsic (Pl) layers (PPL). c) Rounded Opx-Amp and Pl porphyroclasts in a very fine-grained matrix (PPL). d) Cpx porphyroclast showing kinking and undulose extinction in a fine-grained recrystallized matrix of pyroxene, amphibole and plagioclase (XPL). e) Pl porphyroclast showing tapering deformation twins and dynamically recrystallized subgrain boundaries (XPL). f) Rounded Pl and Amp porphyroclasts in a very fine-grained Pl+Amp+Bt±Mgt±Qtz mylonitic matrix of dated sample SJ23P (S: main foliation) (PPL). g) Detail of upper left part of photomicrograph 3 f. Asymmetric strain shadow around plagioclase porphyroclast indicates reverse shear sense (XPL). h) Mylonitic compositional layering (S) transected by minor shear bands (C) showing reverse shear sense (PPL). Amp: amphibole; Cpx: clinopyroxene; Ol: olivine; Opx: orthopyroxene; Pl: plagioclase; Spl: Al-rich spinel. PPL: plane-polarized light, XPL: crossed-polarized light. Scale bar 1 mm in Figs. a), b), d), f), h) and 0.25 mm in Figs. c), e) and g).

exhibit undulose extinction and kinking (Fig. 3d). Chemically, these pyroxenes preserve the same composition than those observed in undeformed metagabbros. Scarce plagioclase porphyroclasts (An₉₉Ab₁, Table 1) exhibit truncated and banded polysynthetic twins, and commonly develop a fine-grained recrystallized rim with similar composition (Fig. 3e). The very fine-grained matrix is mostly composed of polygonal equigranular plagioclase±amphibole, with lesser amounts of pyroxenes, magnetite and ilmenite. No chemical variations have been observed between the mineral compositions of the matrix compared to the porphyroclasts. Fine-grained amphibole+plagioclase+spinel+magnetite aggregates define occasional massive strain shadow structures around polymineralic porphyroclasts and the spinel content decreases in respect to striped domains, with an increase in the magnetite+ilmenite content.

At outcrop scale, in contact with a biotite–garnet mylonitic gneiss, a differentiated leucocratic mylonitized gabbroic lens (e.g. sample SJ23P), a few centimetres wide, displays mostly rounded plagioclase porphyroclasts in a very fine-grained matrix of plagioclase, amphibole, biotite, magnetite and minor quartz (Fig. 3f). Undeformed relic plagioclase porphyroclast cores are more anorthitic (An_{90–86}Ab_{10–14}) than polygonal plagioclase from the recrystallized matrix and along grain boundaries (An_{66–57}Ab_{34–43}). Rounded dark green tschermakitic hornblende, monocrystal porphyroclasts, without any evidence of deformation or recrystallization, are chemically characterized by Al₂O₃ contents ranging from 11.05–12.47 wt.%, Na₂O from 1.02–1.65 wt.% and relatively low TiO₂ (0.41–1.42 wt.%) contents (Table 1). No differences between the amphibole composition of porphyroclasts or matrix are observed, the chemical variations also being dominated by the tschermakitic substitution. Scarce orthopyroxene porphyroclasts (En_{62–60}Fs_{37–39}Wo₁) are present both as individual grains or rimmed by amphibole (Fig. 3c).

Microscopic kinematic indicators in the studied samples are limited to some asymmetric strain shadows around plagioclase, orthopyroxene and amphibole, which indicate reverse shear sense with movement of the hanging wall to the W–SW. Occasional S–C structures, with recrystallized fine-grained amphibole along C bands, suggest a coherent movement (Fig. 3g and h).

5. Geochronology

With the aim of constraining mylonitic deformation, a differentiated mylonitic metagabbro was selected for ⁴⁰Ar/³⁹Ar geochronology. It is composed of plagioclase, amphibole and orthopyroxene porphyroclasts (sample SJ23P). Oval-shaped homogeneous tschermakitic porphyroclasts (Fig. 3f and Table 1) of 350–500 μm diameter were separated from the mylonitic metagabbro. 5–10 amphibole grains (215–180 μm) were irradiated and later analyzed (Table 2) yielding a well-defined plateau age of 432±4 Ma (concordant at the 2σ error level, 91.1% ³⁹Ar released) beginning from the third step in the age-spectrum (Fig. 4a). Ca/K ≈ 8, measured from the ³⁷Ar/³⁹Ar ratio (Fig. 4a) is low for a typical calcic amphibole as a consequence of its relatively high K-content (≈ 1 wt.%, see

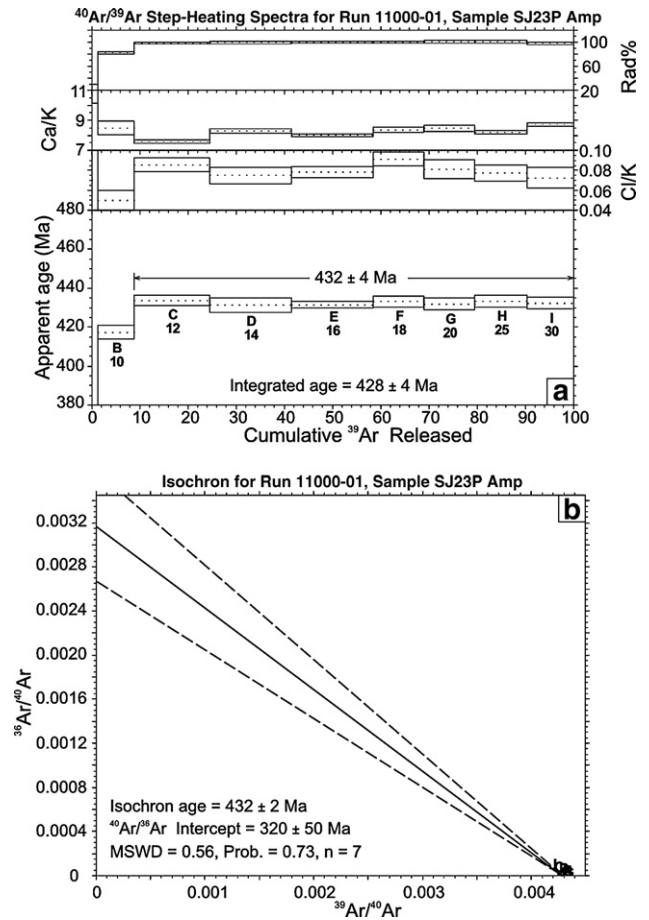


Fig. 4. a) Age spectrum and b) inverse isochron diagram for medium-grade mylonite (sample SJ23P) from Quebrada Sanjuanina, Sierra de La Huerta.

Table 1). The Ca/K ratios obtained in the ⁴⁰Ar/³⁹Ar experiment are very homogeneous, ranging from 7.5 to 9 (Fig. 4a), indicating sample purity of the selected amphibole grains. Low Cl/K ratios indicate the absence of chlorine inclusions. The ³⁶Ar/⁴⁰Ar versus ³⁹Ar/⁴⁰Ar isotope-correlation diagram (Fig. 4b) was plotted using individual steps, and eliminating those steps which show evidence of Ar loss (A and B steps, Table 2). This inverse isochron diagram shows a high concentration of radiogenic argon clustering the data on the abscissa. The slope of the correlation line is defined with a large error and excess argon cannot be consequently detected. However, the obtained isochron age is consistent with the plateau age and the MSWD value (<2) is acceptable.

6. Discussion and conclusions: *P–T–t* geodynamic evolution of the southwestern Gondwana margin

Precise determination of *P–T–t* conditions operating during the crystallization of the basic magmas to generate the mafic and ultramafic rocks is difficult. Petrographic relationships in the igneous mineralogy of the undeformed metagabbros as well as the association of forsteritic olivine and anorthitic plagioclase suggest that pressures at the time of magma crystallization were <6 kbar (Jan and Karim, 1995). The temperature of crystallization of the magma would have been in the range of 950–1150 °C (Fig. 5).

According to the petrographic characteristics of the undeformed and mylonitized metagabbros, four different recrystallization events can be inferred.

6.1. Granulitic stage

Despite the preservation of well-developed metamorphic assemblages, quantitative P – T determination is problematic because of the lack of appropriate (quartz-bearing) mineral assemblages for conventional thermobarometry. The metamorphic reaction involving olivine and plagioclase to produce enstatite+diopside+Al-spinel in coronitic textures (with an absence of garnet) is typical of the medium-pressure granulite facies (5.5–7.5 kbar according to Jan and Karim, 1995, and references therein) and implies diffusion of Fe and Mg from olivine into plagioclase and Si and Ca from plagioclase to olivine (e.g. Indares and Dunning, 1997). Excess of Al in this reaction is used to form Al-spinel when extra Fe and Mg are diffused into the plagioclase (reaction 1 in Fig. 5). Moreover, the absence of garnet in these metagabbros and metagabbro-norites indicates a lack of high-pressure conditions and constrains the maximum P – T conditions (reactions 2 and 3, shadow area in Fig. 5) in which metagabbros could be generated.

T estimations using conventional two-pyroxene equilibrium (clinopyroxene–orthopyroxene in coronas) yielded values of 785–930 °C (Wood and Banno, 1974) and 924–978 °C (Wells, 1977). Nevertheless, these T calculations may be overestimated and values around 850 °C could be more realistic and compatible with petrogenetic grids (e.g. Schmädicke, 2000). With these T values, intersection with the modelled reaction (1) in Fig. 5 gives P values around 7–7.5 kbar. These P – T values, typical of medium-pressure granulites, are similar to those obtained by Jan and Karim (1995) in coronitic metagabbros from the Kohistan island arc and to recent P – T calculations in coronitic metagabbros from Sierra de Valle Fértil, for which values of 7.5–8.5 kbar and 750–850 °C were estimated (Schneider et al., 2006). In any case, the pressure estimation is higher than the magmatic crystallization pressure and is compatible with crustal thickening processes (Fig. 5). Moreover, the anticlockwise P – T path for these mafic granulites (Fig. 5) is controlled by a pressure increase at high temperature. This pattern is normally interpreted as characteristic of active magmatic margins followed by tectonic crustal thickening (e.g. Abati et al., 2003).

Higher P – T metamorphic conditions (12.1 ± 1 kbar and 769 ± 18 °C) were calculated for basement migmatites in the area of Loma de Las Chacras, located on the western flank of the Sierra de La Huerta (Fig. 1), in which U–Pb zircon geochronology defined an age of 463 ± 2 Ma (Baldo et al., 2001). Similar ages of ≈ 460 – 465 Ma have been obtained (Casquet et al., 2001a; Rapela et al., 2001, 2005) for the climax of the regional metamorphism in the Western Sierras Pampeanas. In the Sierra de Las Imanas, Galindo et al. (2004) reported a peak metamorphic age of 464.4 ± 4.5 Ma (Sm–Nd dating) from a migmatitic gneiss which achieved its peak conditions at 6.5–7 kbar and 720–790 °C. Consequently, the medium- P granulitic metamorphism registered in the metagabbros could have

developed around 460–465 Ma, *ca.* 10–30 Ma later than the generation of the Famatinian arc (Fig. 5).

According to Baldo et al. (2001), two different zones with contrasting P/T gradients can be recognized in the Western Famatinian belt. At the westernmost margin of the orogen (Sierra Pie de Palo and Loma de las Chacras), metamorphism is characterized by a relatively high P/T gradient, whereas in central and eastern Sierras de La Huerta–Valle Fértil, metamorphism is characterized by an intermediate P/T gradient. Our P – T values calculated for the granulitic stage are therefore consistent with this proposed thermal model for the Famatinian magmatic belt.

6.2. High-temperature amphibolite facies

The complete $Ol \Rightarrow Opx \pm Spl \Rightarrow Cpx \pm Spl \Rightarrow Amp \pm Spl \Rightarrow Pl$ reaction sequence observed in the coronas (e.g. Fig. 3a) indicates a continuous metamorphic evolution from medium-pressure granulites (water-free with an absence of garnet) to

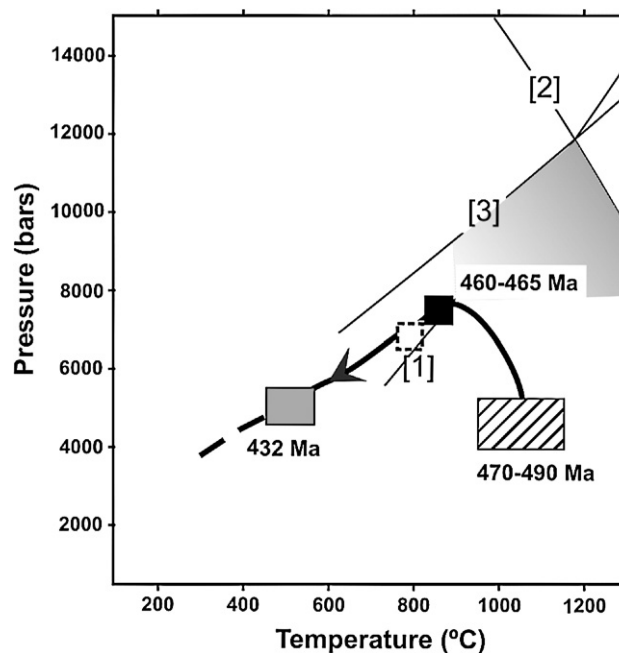


Fig. 5. Metamorphic P – T – t path for the evolution of the metagabbro-norites from the Sierra de La Huerta in the CFMAS system. All metamorphic reactions were calculated using the thermodynamic data and activity models of the TWQ software (Berman, 1991) from microprobe analyses of minerals. [1]: $2Fo + An = Di + 2cEn + Sp$; [2]: $Sp + 4cEn = Fo + Py$; [3]: $2An + 3Fo = Sp + Py + 2Di$. The absence of garnet in the metagabbro-norites is typical of the medium-pressure granulite facies, limiting the P – T conditions to the grey shadow area. For garnet, ideal grossular (Gr) and pyrope (Py) end members were assumed. Hypothetical initial crystallization of gabbros from magma during the development of the Famatinian arc (~ 470 – 490 Ma) is assumed at low-pressures (≤ 6 kbar, 950–1150 °C, streaky rectangle) as suggested by the coexistence of olivine and anorthitic plagioclase (e.g. Jan and Karim, 1995). The granulitic metamorphism (at 460–465 Ma), registered in the $Cpx + Opx + Spl$ coronas would have developed as a consequence of crustal thickening and cooling of gabbros (black square: assumed P – T for medium- P granulite conditions). Dotted white square: assumed P – T conditions for the amphibolite metamorphic facies. Grey rectangle: assumed P – T conditions for mylonitic deformation as deduced from microstructure and amphibole barometry.

upper amphibolite facies conditions (Fig. 5). Applying the Johnson and Rutherford (1989) Al-in amphibole barometer, P values (with an error of ± 0.5 kbar) range from 6 to 7 kbar with an average value of 6.5 kbar. With these P values, estimation of T can be obtained from the Schmädicke petrogenetic grid and values around 800–820 °C are achieved (Fig. 5). The presence of amphibole in the metagabbros is a coupled consequence of decompression and increasing water content.

6.3. High-grade mylonites

The striped microstructure suggests that diffusion processes become more important than the difference in rheology between mafic (pyroxene–amphibole) and felsic (plagioclase) minerals at low differential stress, which indicates high-grade metamorphic conditions during mylonitization (e.g. Passchier and Trouw, 1996). Dynamic recrystallization of pyroxene occurs at medium to high temperatures (Barker, 1994), whereas ductile deformation of plagioclase and amphibole suggests $T > 500$ –650 °C and 650–700 °C, respectively (Gapais, 1989; Berger and Stünitz, 1996). Consequently, a T around 650–700 °C is likely for this high-temperature deformational event. Accepting this temperature range, estimation of pressure based on the Al content of amphibole (Johnson and Rutherford, 1989) could range between 6 and 7 kbar (average 6.5 kbar, Fig. 5).

Generalized mylonitization in the area would have begun at ca. 452–459 Ma (Murra and Baldo, 2001) and has been related to uplift during the later stages of the orogenesis, probably associated with the accretion of the Precordillera terrane to the southwestern Gondwana margin.

6.4. Medium-grade mylonites

In the more leucocratic lenses, the microstructure indicates that deformation occurred at lower temperatures than those reflected by the striped texture. In these mylonites, well preserved porphyroclasts are immersed in a very fine-grained recrystallized matrix. Rounded homogeneous hornblende porphyroclasts, where evidence for internal deformation is absent, reflect a rigid behaviour of major crystals with respect to a finer grained matrix. Plagioclase porphyroclasts display low to medium-temperature plastic deformation, as is suggested by undulose extinction, deformation twinning, bending and grain boundary recrystallization (mantled porphyroclasts). Thus, temperature conditions could be assumed to have been in the order of 400–500 °C for this mylonitic stage (Passchier and Trouw, 1996) and by means of the Al-in amphibole barometry, an average P value of 5.2 kbar (ranges from 4.7 to 5.7 kbar) is obtained (Fig. 5).

The closure temperature of hornblende to retain Ar (around 450–550 °C, e.g. Mc Dougall and Harrison, 1999) is close to the temperature inferred from the deformation conditions for the lower temperature mylonitization event in the study area (Fig. 5). In fact, the plateau age at 432 ± 4 Ma for the amphibole porphyroclasts suggests that their Ar systematics were totally reset during the amphibolite facies mylonitization event because these amphiboles were initially formed at ~ 468 –499 Ma (age of gabbro protolith). Therefore, the plateau age at 432 ± 4 Ma is

interpreted as the best estimate for the age of the medium-grade mylonitization event, providing evidence that tectonic activity was taking place in the Early Silurian.

Coeval mylonitic deformation has been demonstrated by Ramos et al. (1996, 1998) and Casquet et al. (2001b) in different basement lithologies of the Sierra Pie de Palo and Cerro Barboza, west of the studied area. Cooling ages (Ar/Ar on muscovite) of the last episode of ductile deformation and uplift ranging between 432 and 394 Ma indicate the cessation of ductile deformation in the Pie de Palo region (Ramos et al., 1998). The origin of these ductile shear zones has been assumed by Ramos et al. (1998) to be associated with the last thrusting and subsequent uplift processes related to the collision episodes between the Cuyania terrane and the proto-margin of Gondwana.

The coincidence in radiometric ages of the mylonitization events in the Sierra Pie de Palo and Sierra de la Huerta using minerals with different closure temperatures, could suggest a common post-collisional history (with a different rate of cooling or exhumation) of these two Sierras Pampeanas areas in the evolution of the Gondwana margin during Early Silurian time. Moreover, structural and petrological differences observed between the Sierra de Valle Fértil, Sierra de la Huerta and Sierra de Las Imanas (northern, central and southern parts of the belt), reflect different structural levels of the Famatinian arc. The abundance of mafic and ultramafic rocks in the Sierra de la Huerta is interpreted as belonging to the roots of the arc and, consequently, the P – T conditions obtained for rocks from this area could be different from those obtained at other structural levels.

Acknowledgments

The authors thank the reviewers J. Abati, E. Baldo, C. Casquet, A. Iriondo and M. Santosh for their constructive and helpful comments and suggestions, which significantly improved the quality of the initial manuscript. Dr. J. Le Roux and Geol. Andrew Hodgkin are acknowledged for reviewing the English. This research was funded by PIP-5649 Project, CONICET, Argentina.

References

- Abati, J., Arenas, R., Martínez Catalán, J.R., Díaz García, F., 2003. Anticlockwise P – T path of granulites from the Monte Castelo Gabbro (Órdenes Complex, NW Spain). *Journal of Petrology* 44 (2), 305–327.
- Arancibia, G., Matthews, S., Pérez de Arce, C., 2006. K–Ar and $^{40}\text{Ar}/^{39}\text{Ar}$ geochronology of supergene processes in the Atacama Desert, northern Chile: tectonic and climatic relations. *Journal of the Geological Society (London)* 163, 107–118.
- Astini, R.A., Benedetto, J.L., Vaccari, N.E., 1995. The Early Paleozoic evolution of the Argentine Precordillera as a Laurentian rifted, drifted, and collided terrane: a geodynamic model. *Geological Society of America Bulletin* 107, 253–273.
- Baldo, E., Casquet, C., Rapela, C., Pankhurst, R., Galindo, C., Fanning, C.M., Saavedra, J., 2001. Ordovician metamorphism at the southwestern margin of Gondwana: P – T conditions and U–Pb SHRIMP ages from Loma de Las Chacras, Sierras Pampeanas. III South American Symposium on Isotope Geology, pp. 544–547. Pucón, Chile. CD-ROM edition.
- Barker, A.J., 1994. *Introduction to Metamorphic Textures and Microstructures*. Blackie Academic & Professional, Oxford. 170 pp.

- Berger, A., Stünitz, H., 1996. Deformation mechanisms and reaction of hornblende: examples from the Bergell tonalite (Central Alps). *Tectonophysics* 257, 149–174.
- Berman, R.G., 1991. Thermobarometry using multiequilibrium calculations: a new technique with petrological applications. *Canadian Mineralogist* 29, 833–855.
- Casquet, C., Baldo, E.G., Pankhurst, R.J., Rapela, C.W., Galindo, C., Fanning, C.M., Saavedra, J., 2001a. Involvement of the Argentine Precordillera in the Famatinian mobile belt; geochronological (U–Pb SHRIMP) and metamorphic evidence from the sierra de Pie de Palo. *Geology* 29, 703–706.
- Casquet, C., Baldo, E.G., Pankhurst, R.J., Rapela, C.W., Galindo, C., Fanning, C.M., Saavedra, J., 2001b. Thermochronology of Famatinian metamorphism at the eastern margin of the Precordillera terrane. XI Congreso Latinoamericano de Geología, Montevideo. Proyecto IGCP, vol. 436, p. 163. CD-ROM edition.
- Castro de Machuca, B., Conte-Grand, A., Meissl, E., Pontoriero, S., Sumay, C., 1996. Petrología de las asociaciones máficas-ultramáficas de la sierra de La Huerta, San Juan, Argentina. XIII Congreso Geológico Argentino y III Congreso de Exploración de Hidrocarburos, vol. III, pp. 439–452. Buenos Aires.
- Castro de Machuca, B., Conte-Grand, A., Meissl, E., Pontoriero, S., Recio, G., Sumay, C., 2002. Mineralogy and textures of metagabbros and ultramafic related rocks from La Huerta and Valle Fértil ranges, Western Pampean range, San Juan, Argentina. In: de Brodtkorb, M.K., Koukharsky, M., Leal, P.R. (Eds.), *Mineralogía y Metalogenia 2002*, VI Congreso de Mineralogía y Metalogenia, pp. 67–75. Buenos Aires.
- Castro de Machuca, B., Morata, D., Arancibia, G., Belmar, M., Pontoriero, S., 2004. Metamorphic evolution of high-grade metagabbros from La Huerta range, Western Pampean Ranges, San Juan, Argentina. 32nd Int. Geol. Congr., Abs. vol. 1, abs. 29–13, p. 152. Florence, Italy.
- Castro de Machuca, B., Arancibia, G., Morata, D., Belmar, M., Pontoriero, S., Previley, L., 2005. Transformaciones texturales, mineralógicas y químicas en metagabros afectados por cizallamiento dúctil, sierra de La Huerta, San Juan, Argentina. In: Llambías, E., de Barrio, R., González, P., Leal, P. (Eds.), XVI Congreso Geológico Argentino, Actas, vol. I, pp. 907–914. La Plata.
- Chernicoff, C.J., Ramos, V., 2003. El basamento de la sierra de San Luis: nuevas evidencias magnéticas y sus implicancias tectónicas. *Revista de la Asociación Geológica Argentina* 58 (4), 511–524.
- Dahlquist, J., Pankhurst, R., Rapela, C., Casquet, C., Fanning, C., Alasino, P., Báez, M., 2006. The San Blas Pluton: an example of Carboniferous plutonism in the Sierras Pampeanas, Argentina. *Journal of South American Earth Sciences* 20, 341–350.
- Galindo, C., Murra, J., Baldo, E., Casquet, C., Rapela, C.W., Pankhurst, R.J., Dahlquist, J., 2004. Datación Sm–Nd del metamorfismo en la Sierra de las Imanas (Sierras Pampeanas Occidentales, Argentina). *Geogaceta* 35, 75–78.
- Gapais, D., 1989. Shear structures within deformed granites: mechanical and thermal indications. *Geology* 17, 1144–1147.
- Indares, A., Dunning, G., 1997. Coronitic metagabbro and eclogite from the Grenville Province of western Quebec: interpretation of U–Pb geochronology and metamorphism. *Canadian Journal of Earth Sciences* 34, 891–901.
- Introcaso, A., Martínez, M., Giménez, M., Ruiz, F., 2004. Geophysical study of the Valle Fértil lineament between 28° 45' S and 31° 30' S: boundary between the Cuyania and Pampia terranes. *Gondwana Research* 7 (4), 1117–1132.
- Jan, M.Q., Karim, A., 1995. Coronas and high-*P* veins in metagabbros of the Kohistan island arc, northern Pakistan: evidence for crustal thickening during cooling. *Journal of Metamorphic Geology* 13, 357–366.
- Johnson, M.C., Rutherford, M.J., 1989. Experimental calibration of the aluminium-in-hornblende geobarometer with application to Long Valley Caldera (California) volcanic rocks. *Geology* 17 (9), 837–841.
- Keller, M., Buggisch, W., Lehnert, O., 1998. The stratigraphical record of the Argentina Precordillera and its plate-tectonic background. In: Pankhurst, R.J., Rapela, C.W. (Eds.), *The proto-Andean Margin of Gondwana*. Special Publication, vol. 142. Geological Society, London, pp. 35–56.
- Kleine, T., Mezger, K., Zimmermann, U., Münker, C., Bahlburg, H., 2004. Crustal evolution along the Early Ordovician Proto-Andean margin of Gondwana: trace element and isotopic evidence from the Complejo Igneo Pocitos (Northwest Argentina). *The Journal of Geology* 112, 503–520.
- Mc Dougall, I., Harrison, T., 1999. *Geochronology and Thermochronology by the ⁴⁰Ar/³⁹Ar Method*, 2nd ed. Oxford University Press. 269 pp.
- Murra, J., 2004. Estudio petrológico-estructural del borde occidental del orógeno Famatiniano (Sierras de Valle Fértil-La Huerta) y su comparación con el sector central (Sierras de Las Minas-Ulapes), provincias de San Juan y La Rioja. PhD Thesis, Universidad Nacional de Córdoba, Argentina, 329 pp.
- Murra, J., Baldo, E., 2001. Metamorfismo y deformación en la sierra de Las Imanas, margen occidental del cinturón famatiniano, Sierras Pampeanas Argentinas. XI Congreso Latinoamericano de Geología, Trabajo, vol. 110. Montevideo, Uruguay. CD-ROM edition.
- Murra, J., Baldo, E., 2006. Evolución tectonotermal ordovícica del borde occidental del arco magmático Famatiniano: metamorfismo de las rocas máficas y ultramáficas de la Sierra de La Huerta-de Las Imanas (Sierras Pampeanas, Argentina). *Revista Geológica de Chile* 33, 277–298.
- Pankhurst, R.J., Rapela, C.W., 1998. The proto-Andean Margin of Gondwana: an introduction. In: Pankhurst, R.J., Rapela, C.W. (Eds.), *The proto-Andean Margin of Gondwana*. Special Publication, vol. 142. Geological Society, London, pp. 1–9.
- Pankhurst, R.J., Rapela, C.W., Saavedra, J., Baldo, E.G., Dahlquist, J., Pascua, I., Fanning, C.M., 1998. The Famatinian magmatic arc in the central Sierras Pampeanas: an Early to Mid-Ordovician continental arc on the Gondwana margin. In: Pankhurst, R.J., Rapela, C.W. (Eds.), *The proto-Andean Margin of Gondwana*. Special Publication, vol. 142. Geological Society, London, pp. 343–367.
- Pankhurst, R.J., Rapela, C.W., Fanning, C.M., 2000. Age and origin of coeval TTG, I- and S-type granites in the Famatinian belt of NW Argentina. *Transactions of the Royal Society of Edinburgh, Earth Sciences* 91, 151–168.
- Passchier, C.W., Trouw, R.A.J., 1996. *Microtectonics*. Springer, Germany. 189 pp.
- Rabbia, O., 1996. The gabbroic rocks of Sierra de Valle Fértil, Western Sierras Pampeanas: an advective heat source for high grade metamorphism and migmatization? XIII Congreso Geológico Argentino y III Congreso de Exploración de Hidrocarburos, Actas, vol. V, p. 561. Buenos Aires.
- Ramos, V., 1988. Late Proterozoic–Early Palaeozoic of South America. A collisional history. *Episodes* 11, 168–175.
- Ramos, V., 2004. Cuyania, an exotic block to Gondwana: review of a historical success and the present problems. *Gondwana Research* 7 (4), 1009–1026.
- Ramos, V., Jordan, T., Allmendinger, R., Mpodozis, C., Kay, S., Cortés, J., Palma, M., 1986. Paleozoic terranes of the Central Argentine–Chilean Andes. *Tectonics* 5, 855–880.
- Ramos, V., Vujovich, G., Dallmeyer, R., 1996. Los klippen y ventanas tectónicas preándicas de la sierra de Pie de Palo (San Juan): edad e implicaciones tectónicas. XIII Congreso Geológico Argentino y III Congreso de Exploración de Hidrocarburos, vol. V, pp. 377–391. Buenos Aires.
- Ramos, V., Dallmeyer, R., Vujovich, G., 1998. Time constraints on the Early Paleozoic docking of the Precordillera, central Argentina. In: Pankhurst, R.J., Rapela, C.W. (Eds.), *The proto-Andean Margin of Gondwana*. Special Publication, vol. 142. Geological Society, London, pp. 143–158.
- Rapela, C., Pankhurst, R., Casquet, C., Baldo, E., Saavedra, J., Galindo, C., 1998. Early evolution of the proto-Andean margin of South America. *Geology* 26, 707–710.
- Rapela, C., Pankhurst, R., Baldo, E., Casquet, C., Galindo, C., Fanning, C.M., Saavedra, J., 2001. Ordovician metamorphism in the Sierras Pampeanas: new U–Pb SHRIMP ages in central-east Valle Fértil and the Velazco batholith. III South American Symposium on Isotope Geology, pp. 616–619. Pucón, Chile. CD-ROM edition.
- Rapela, C., Pankhurst, R.J., Casquet, C., Fanning, C.M., Galindo, C., Baldo, E., 2005. Datación U–Pb SHRIMP de circones detríticos en parafibrolitas neoproterozoicas de la secuencia Difunta Correa (Sierras Pampeanas Occidentales, Argentina). *Geogaceta* 38, 227–230.
- Schmädicke, E., 2000. Phase relations in peridotitic and pyroxenitic rocks in the model systems CMASH and NCMASH. *Journal of Petrology* 41, 69–86.
- Schneider, I., Mogessie, A., Gallien, F., Castro de Machuca, B., Bjerg, E.A., Delpino, S., Previley, L., Pontoriero, S., Meissl, E., Kostadinoff, J., 2006. Coronitic gabbros and associated basement rocks of the Valle Fértil–La Huerta Ranges, San Juan Province, NW Argentina. *Pangeo Austria 2006*, Conference Series. Innsbruck University Press, pp. 316–317.
- Thomas, W.A., Astini, R.A., 1996. The Argentine Precordillera: a traveller from the Ouachita embayment of North American Laurentia. *Science* 273, 752–757.

- Vujovich, G., Godeas, G.M., Pezzutti, N., 1996. El complejo magmático de la sierra de la Huerta, provincia de San Juan. *Actas XIII Congreso Geológico Argentino y III Congreso de Exploración de Hidrocarburos*, vol. III, pp. 465–475. Buenos Aires.
- Vujovich, G., van Staal, C.R., Davis, W., 2004. Age constraints on the tectonic evolution and provenance of the Pie de Palo Complex, Cuyania Composite Terrane, and the Famatinian Orogeny in the Sierra Pie de Palo, San Juan, Argentina. *Gondwana Research* 7 (4), 1041–1056.
- Wells, P.R.A., 1977. Pyroxene thermometry in simple and complex systems. *Contributions to Mineralogy and Petrology* 62, 129–139.
- Wood, B.J., Banno, S., 1974. Garnet–orthopyroxene and orthopyroxene–clinopyroxene relationships in simple and complex systems. *Contributions to Mineralogy and Petrology* 42, 109–124.